Fourier spectroscopy of a spin-orbit coupled Bose gas

Ana Valdés-Curiel, Dimitri Trypogeorgos, Erin E. Marshall, Ian B. Spielman

Joint Quantum Institute, University of Maryland and National Institute of Standards and Technology, College Park, Maryland, 20742, USA

Abstract.

We propose a time domain technique to measure the band structure of a spin-1 spin-orbit coupled Bose-Einstein condensate that relies on the Hamiltonian evolution of the system. We drive transitions at different values of detuning from Raman resonance and extract the Fourier components of the time dependent evolution to reconstruct the spin and momentum dependent energy spectrum. We add a periodic modulation to one Raman field which results in a tunable spin-orbit coupling dispersion and a spectrum of Floquet quasi-energies that we can directly measure, showing the robustness of our technique.

1. Introduction

Properties of materials deeply depend in their underlying band structure. Cold atoms offer engineering single particle dispersions that are analogues to condensed matter systems and new exotic materials, e.g. completely flat bands where interactions dominate the system, spin-orbit coupling. The ability to measure and control leads to new understanding and paves the way to access new phases of matter.

Spinorbit (SO) coupling is an essential mechanism for most spintronics devices and leads to many fundamental phenomena in condensed matter physics and atomic physics. For example, SO coupling gives rise to the quantum spin Hall effect in electronic condensed matter systems quantum Hall effect, Floquet topological insulators, etc.

The relation between the dynamics of a system and its energy spectrum is rooted in the heart of quantum mechanics. This relation has been exploited before to study properties of both condensed mattter (una cita aqui) and cold atoms systems (otra cita) alike. Here, we propose a new Fourier spectroscopy technique to measure the dispersion relation of a system of spin-one, spin-orbit coupled ultra-cold atoms, which unlike previously studied techniques, relies only in the Hamiltonian evolution of the system and does not require any additional hardware or hyperfine states. This techniques works because when an atomic bare eigenstate is projected into a superposition of dressed states when a field is suddenly turned on, and will continue to evolve and Rabi oscillate in time, with spectral components related to the relative energies of the dressed states.

We generate spin-orbit coupling in a spin-one atom using a pair of 'Raman' laser beams that change the spin state while imparting momentum to a spin-one atom via two photon Raman transitions.

A uniform magnetic field $B\hat{\mathbf{e}}_z$ generates a linear Zeeman splitting of the energy levels $\hbar\omega_Z = g_F\mu_B B$, where μ_B is the Bohr magneton and g_F is the Landé g factor, and introduces a quadratic Zemen shift ϵ that shifts the energy of the $|m_F = 0\rangle$ state with respect to the $|m_F = \pm 1\rangle$ states. We couple these states using a pair of intersecting, cross polarized Raman beams with a wavelength $\lambda_R = 790.024$ nm. We offset the frequency of the lasers by $\delta\omega = \omega_Z + \Delta_0$, where Δ_0 is an experimentally controllable detuning from four photon resonance between the $|m_F = -1\rangle$ and $|m_F = +1\rangle$ states.

The Raman field couples the state $|m_F = 0,\ q_x\rangle$ to $|m_F = -1,\ q_x + 2k_L\rangle$ and to $|m_F = +1,\ q_x - 2k_L\rangle$, generating a spin change of $\delta m_F = \pm 1$ and imparting a shift in momentum of $\pm 2k_L$, where q_x denotes the quasimomentum. The geometry and wavelength of the Raman field determine the natural units of the system: the single photon recoil momentum $k_L = \frac{2\pi}{\lambda_R}\sin(\theta/2)$ and its associated recoil energy $E_L = \frac{\hbar^2 k_L^2}{2m}$.

In a frame rotating at a frequency ω_Z, and after a rotating wave approximation, the kinetic and atom-light contributions of the Hamiltonian along the recoil direction are

$$\begin{aligned}\hat{H}_x =& \frac{\hbar^2\hat{q}_x^2}{2m} + \alpha_0\hat{q}_x\hat{F}_z + 4E_L\mathbb{I} + \frac{\Omega_R}{2}\hat{F}_x\Big] \\ &+ (-\epsilon + 4E_L)(\hat{F}_z^2 - \mathbb{I}) + \Delta_0\hat{F}_z,\end{aligned} \tag{1}$$

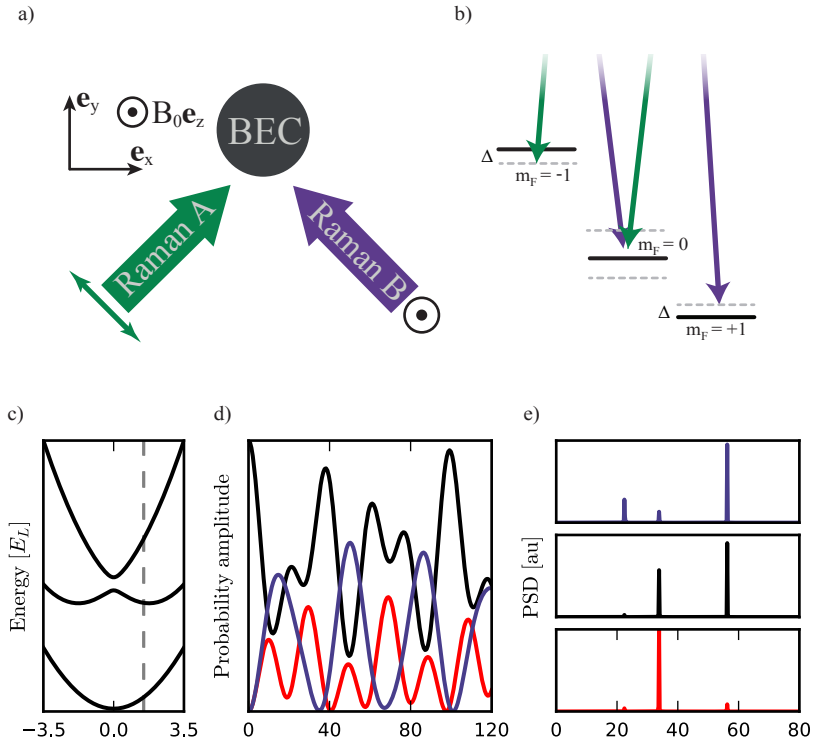

Figure 1. **c)** SOC dispersion of a spin-one system with quadratic Zeeman shift of $9E_L$ and Raman coupling $\Omega_0 = 12E_L$, initially prepared at a momentum $k_x = 2k_L$. **d)** Probability amplitude of measuring the atoms in the state $|m_F = -1,\ q_x = q_x + 2k_L\rangle$ (red), $|m_F = 0,\ q_x = q_x\rangle$ (black), and $|m_F = +1,\ q_x = q_x - 2k_L\rangle$ (blue) as a function of Raman pulsing time. **e)** Fourier transform of the probability amplitude. The three peaks in the Fourier spectra correspond to the three relative energies in the SOC dispersion for the parameters described above.

where $\hat{F}_{x,y,z}$ are the spin-one matrices, $\alpha_0 = \frac{\hbar^2 k_L}{m}$ is the spin-orbit coupling strength, $\Omega_R \propto E_A^\star E_B$ and the Raman coupling strength which is proportional to the field intensity.

Figure 1a shows the typical band structure as a function of quasimomentum that results after diagonalizing the Hamiltonian $\hat{H}_x$ for a negative quadratic Zeeman shift $|\epsilon| > 4E_L$. The ground state band is pushed down with respect to the higher excited bands, and it can be well described by a harmonic potential as there are no crossings with the higher bands.

1.1. Fourier spectroscopy of spin-orbit coupled atoms

We can directly measure the dispersion relation of a system of spin-one, spin-orbit coupled bosonic atoms by studying the Hamiltonian evolution of the system, and unlike previous measurements of a SOC dispersion, our technique does not require any additional hardware.

We start with bare atoms in the $|m_F = 0,\ k_x\rangle$ state. When a Raman field is

suddenly turned on, the initial state is projected into the Raman dressed state basis, and continues to evolve $|m_F = 0, q_x\rangle \rightarrow \sum_{i=1}^{3} c_i e^{i\omega_i t}|\psi_i\rangle$, where $\omega_i = E_i/\hbar$ are the angular frequencies associated to the dressed state energies and $|\psi_i\rangle$, the dressed eigenstates, are linear combinations of $|m_F = 0,\ q_x = k_x\rangle$ and $|m_F = \pm 1,\ q_x = k_x \mp 2k_L\rangle$. We then turn off the Raman field and image the atoms, which projects the system back into the bare basis $|m_F = 0,\ q_x = k_x\rangle$, $|m_F = \pm 1,\ q_x = k_x \mp 2k_L\rangle$. The probability amplitude of measuring atoms in an m_F state after evolving for a time t oscillates at frequencies given by the difference in the dressed state energies $P_{m_F}(t) = \sum_{i \neq j} 2c_{ij} \cos((\omega_i - \omega_j)t)$.

The Fourier spectroscopy technique relies in directly measuring the probability amplitude as a function of evolution time and extracting the relative energies of the system using a Fourier transform, as shown in figure 1.

The method described above so far only allows us to measure relative energies and we must add a known energy reference if we want to recover the dispersion relation. We can do so by measuring the effective mass $m^\star = \hbar^2[\frac{d^2E(k_x)}{dk_x}]^{-1}$ of the nearly quadratic lowest branch of the dispersion, and then shifting the measured frequencies accordingly.

We can map the full spin and momentum dependent band structure of the spin-orbit coupled system by repeating this procedure for different initial momentum states, however, it may not be as straightforward to reliably prepare an arbitrary momentum state in the lab. The measurement however can be simplified by noticing that a non-moving atom cloud in the laboratory reference frame dressed by a field with non-zero detuning is equivalent to a moving cloud with a resonant field in a moving reference frame. This can be explicitly seen in the Hamiltonian 1 by looking at the detuning term $\Delta_0 \hat{F}_z$ and the momentum term $\alpha_0 \hat{q}_x \hat{F}_z$, which have the same effect in the relative energies. There is an additional Doppler shift associated with the transformation between reference frames, which gets canceled when we look at the energy differences. Therefore, for the purpose of our experiments, momentum and detuning are equivalent up to a numerical factor: $\Delta_0/E_R = 4q_x/k_R$, and we can measure by preparing a zero momentum state and measuring the probability amplitude for different values of Raman detuning Δ_0.

1.2. Spectroscopy of a driven system

A time evolution based spectroscopy is ideal to study the energy spectrum of more complex time dependent systems. A particularly interesting case is that of periodically driven systems [cita aqui], which can be described by effective coupling terms in the Hamiltonian that arise from averaging the fast dynamics of the system. The Fourier spectroscopy technique can be applied to such systems to measure the Floquet quasi-energy spectrum and also study the couplings within different Floquet manifolds.

We will focus on the case of a spin-1 spin-orbit coupled system that is coupled by a multiple frequency Raman field, as shown in Fig 3b. The interference of the multiple frequencies leads to a periodic amplitude modulation in the field and an effective Floquet Hamiltonian that has tunable spin-orbit coupling.

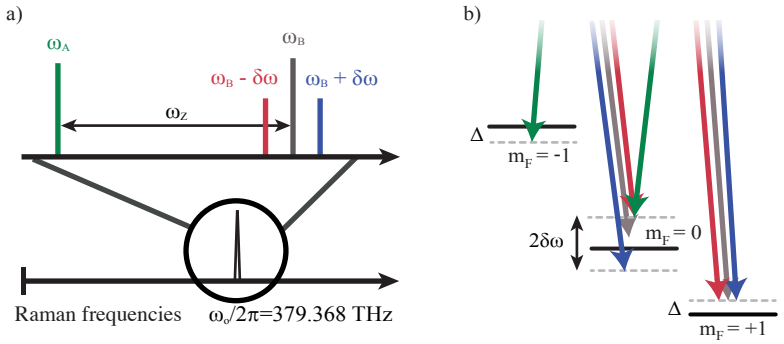

Figure 2. Time evolution of the BEC for Raman pulsing times between 5 and 10 μs, for different spin orbit coupling regimes: **(i)** $\Omega_0 = 9.9E_L$, $\Omega = 04$, $\Delta = 5.8E_L$, **(ii)** $\Omega_0 = 0$, $\Omega = 8.6E_L$, $\Delta = -0.7E_L$, and **(iii)** $\Omega_0 = 1.5E_L$, $\Omega = 8.4E_L$, $\Delta = -4.7E_L$

We add two sidebands to one Raman beam at angular frequencies $\omega = \omega_L + \omega_Z + \Delta_0 \pm \delta\omega$. The Hamiltonian in Eq.1 remains unchanged, except for the coupling strength that takes the form $\Omega_R(t) = \Omega_0 + \Omega\cos(\delta\omega t)$. Our periodically driven system is well described by Floquet theory: the eigenstates are of the form $|\Psi(t)\rangle = \sum_j c_j e^{i\epsilon_j t}|u_j(t)\rangle$ where $|u(t)\rangle$ are time-periodic states and the ϵ_j are the Floquet quasi-energies, wich are $\epsilon_j, n = \epsilon_{j,m} + (n-m)2\pi/T$

The time evolution of the system after one driving cycle can be described in terms of an effective time-independent Hamiltonian $e^{iT\hat{H}_{eff}}$. If $\delta\omega \gg \epsilon$ and $\delta\omega \gg 4E_L$, this effective Floquet Hamiltonian retains the form of 1 with renormalized coefficients, and an additional term that couples the $m_f = -1$ and $m_f = +1$ states:

$$\begin{aligned}\hat{H} =& \frac{\hbar^2\hat{k}^2}{2m} + \alpha\hat{k}\hat{F}_z + 4E_L\mathbb{I} + \frac{\Omega_0}{2}\hat{F}_x \\ &+ \frac{\tilde{\Omega}}{2}\hat{F}_{xz} + (\tilde{\epsilon} + 4E_L)(\hat{F}_z^2 - \mathbb{I}) + \tilde{\Delta}\hat{F}_z,\end{aligned} \tag{2}$$

with $\alpha = J_0(\Omega/2\delta\omega)\alpha_0$, $\tilde{\Omega} = \frac{1}{4}(\epsilon + 4E_L)(J_0(\Omega/\delta\omega) - 1)$, $\Delta = J_0(\Omega/2\delta\omega)\Delta_0$, and $\tilde{\epsilon} = \frac{1}{4}(4E_L - \epsilon) - \frac{1}{4}(4E_L + 3\epsilon)J_0(\Omega/\delta\omega)$, and J_0 the zeroth order Bessel function of the first kind.

If the quadratic Zeeman shift and the amplitude modulation are large compared to the recoil energy $|\epsilon|, \delta\omega > 4E_L$, the Hamiltonian described above can be approximated by an effective spin 1/2, spin-orbit coupled system,with tunable spin-orbit coupling: the state $|m_F = +1,\ q_x = k_x - 2J_0(\Omega/2\delta\omega)k_R\rangle$ is coupled to the $|m_F = -1,\ q_x = k_x + 2J_0(\Omega/2\delta\omega)k_R\rangle$ with coupling strength $\Omega' = \tilde{\Omega} + \hbar\Omega_0^2/2\tilde{\epsilon}$.

This model is good to describe the energies within one Floquet manifold, however, if the coupling strength is large compared to the quadratic Zeeman shift Ω_0, $\Omega < \epsilon$, rotating wave type approximations break down, and the time evolution of the system becomes more complex. A signature of this is the appearance of higher frequency Fourier

components in the probability amplitude, spaced by $2n\pi/T$ from the lowest 3 energy levels.

2. Experiment

We are interested in measuring the SOC dispersion for three different types of coupling schemes: (i) A time independent spin-orbit coupled system, $\Omega_0 \neq 0$ and $\Omega = 0$, (ii) for a periodically driven spin-orbit coupled system with no DC offset $\Omega \neq 0$ and $\Omega_0 = 0$, and (iii) A time periodically driven spin-orbit coupled system with a DC offset $\Omega \neq 0$ and $\Omega_0 \neq 0$.

2.1. Spectroscopy experimental sequence

We start our experiments with a Rb^{87} Bose-Einstein condensate (BEC) with $N \approx 4\times10^4$ (measure) atoms in the $|F = 1, m_F = 0\rangle$ state, confined in a 1064 nm crossed optical dipole trap, with trapping frequencies $(\omega_x, \omega_y, \omega_z) = 2\pi(42(3), 34(2), 133(3))$ Hz. We break the degeneracy between the m_F magnetic sub-levels by applying a 17.0556 G bias field along the z axis, which produces a Zeeman splitting of 12 MHz and a quadratic Zeeman shift that lowers the energy of the $|F = 1, m_F = 0\rangle$ state by 20.9851 kHz. We adiabatically prepare our BEC in the $|m_F = 0\rangle$ by slowly ramping the bias field while applying a 14 MHz radio-frequency field. We then apply a pair of microwave pulses that serve to monitor and stabilize the bias field and. We generate spin-orbit coupling between the magnetic sub levels with a pair of intersecting, cross-polarized Raman beams, with wavelength $\lambda = 790.33nm$ propagating along $\mathbf{e}_x + \mathbf{y}$ and $\mathbf{e}_x - \mathbf{e}_y$ as shown in Fig 1a. We offset the frequency of the beams using two acusto optic modulators (AOMs), one of them driven by a superposition of up to three different frequencies. On resonance, the laser frequencies satisfy the condition $\omega_A - \omega_B = \omega_A - \frac{\omega_{B+}+\omega_{B-}}{2} = \omega_Z$, and we change the Raman detuning Δ_0 by keeping the magnetic field constant and changing the value of the frequency ω_A.

To get our probability amplitude measurements, we keep the detuning value Δ_0 fixed and pulse the Raman beams on for time intervals between 5 μs and up to 900 μs. For the time independent SOC measurements (case (i)) we take a total of 120 different pulses, for the periodically driven SOC measurements (cases (ii) and (iii)) which require better resolution and bandwidth, we take a total of 180 pulses. After pulsing the Raman we release the atoms from the optical dipole trap and let them fall for a 21 ms time of flight (TOF) time before and apply a spin-dependent force using magnetic field gradient. Our absorption images reveal the atoms spin and momentum distribution, from which we can extract the probability amplitudes by counting the number of atoms in each spin and quasimomentum state: $P(m_F, t) = \frac{n(m_F,t)}{n(m_F=+1,t)+n(m_F=0,t)+n(m_F=-1,t)}$. We repeat this procedure for values of Raman detuning within the interval $\pm12E_L$ which corresponds to quasimomentum values within $\pm3k_L$.

The time dependent SOC measurements additionally required phase stability

between the 3 frequency components in the Raman B field. We set all the relative phases to zero at the beginning of each pulse and kept it constant throughout our experiments. We made the choice of zero relative phase as it maximizes the effective couplings Ω and Ω_0 for a given field intensity. For a more detailed discussion of the effect of the relative phases see the Appendix section.

2.2. Effective mass measurement

We measure the atom's ground state effective mass by inducing dipole oscillations in our BECs for both the bare and Raman dressed atoms. The effective mass $m^\star$ of the dressed atoms is related to the bare mass m and the bare and dressed trapping frequencies ω and ω^star by the ratio $m^\star/m = \sqrt{\omega^\star/\omega}$

To measure the trapping frequencies, we prepare our system in the $|m_F = 0,\ k_x = 0\rangle$ and adiabatically turn on the Raman in ≈ 10 ms while also ramping the detuning to a non-zero value, around $0.5E_R$. Our system does not have the capability to dynamically change the laser frequency while maintaining phase stability, so unlike the pulsing experiments, we ramped the magnetic field to change the resonance conditions. This detuning shifts the minima in the ground state energy away from zero quasi-momentum. We then suddenly snap the field back to resonance which changes the equilibrium conditions of the system and excites the dipole mode of our optical dipole trap. To measure the bare state frequency, we use the Raman beams to initially excite the dipole mode of the trap but we quickly turn on the field (~ 1 ms) and let the BEC continue to oscillate in the unmodified dipole potential.

For this set of measurements we modified our trapping frequencies to $(\omega_x, \omega_y, \omega_z) = 2\pi(35.9, 32.5, xx)$ Hz so that they were nominally symmetric along the $x - y$ plane.

2.3. Magnetic field stabilization

We stabilized the magnetic field and measured fluctuations about the desired set point by applying a pair of microwave pulses with frequencies close to resonance from the $5^2S_{1/2}$ $F = 2$ state, and imaging the in-situ the population transfered by each pulse.

We first prepare our BEC in the $|F = 1, m_f = 0\rangle$ state and apply a 17.0556 G bias filed along the z axis. We then apply a pair of $250\mu s$ microwave pulses close to $6.83GHz$ that transfers about 10% of the atoms into the $F = 2$ manifold. The pulses were detuned by ± 2 kHz from the $|F = 1, m_F = 0\rangle \leftrightarrow |F = 2, m_F = 1\rangle$ transition and were spaced in time by 2 periods of 60 Hz. We image the atoms transfered into $F = 2$ non-destructively using absorption imaging without repumping light. The imbalance in the number of atoms transferred by each pulse gives us a 4 kHz wide error signal that we use both to feed forward our bias coils for active field stabilization, and also to keep track of the magnetic fields at each shot. We trigger our sequence to the line and both the microwave and Raman pulses are timed at integer periods of 60 Hz and performed at the zero-derivative point of the 60 Hz curve in order to minimize additional magnetic field fluctuations

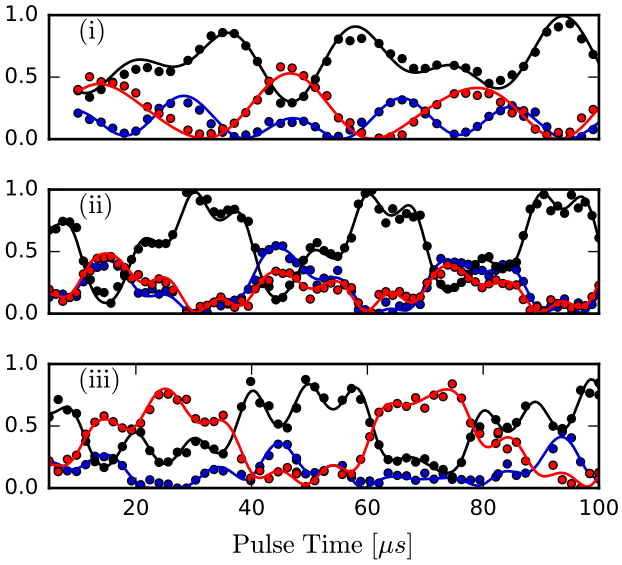

Figure 3. Time evolution of the BEC for Raman pulsing times between 5 and 10 μs, for different spin orbit coupling regimes: **(i)** $\Omega_0 = 9.9E_L$, $\Omega = 04$, $\Delta = 5.8E_L$, **(ii)** $\Omega_0 = 0$, $\Omega = 8.6E_L$, $\Delta = -0.7E_L$, and **(iii)** $\Omega_0 = 1.5E_L$, $\Omega = 8.4E_L$, $\Delta = -4.7E_L$

3. Results

We studied the time evolution for three different schemes of SOC. We calibrated the Raman coupling terms Ω and Ω_0 and the detuning from Raman resonance Δ by fitting the three-level Rabi oscillations of the $|m_F = 0\rangle$ and $|m_f = \pm 1\rangle$ states to the time evolution given by the Hamiltonian in Eq. 1. Figure 3 shows representative traces for the time evolution of our system for the three cases outlined above. These calibrations along with the information gained from the images of atoms out-coupled with microwaves guaranteed that we were indeed at the correct detuning from Raman resonance and that the Raman coupling strength remained nominally constant throughout our measurements.

The time evolution shows higher frequency components for cases (ii) and (iii), as expected from the Floquet quasi-energy spectrum, since the Raman coupling strength Ω, Ω_R is comparable to the quadratic Zeeman shift ϵ.

To calculate the effective mass we fitted sinusoids to the sloshing motion of our atoms in the dipole trap and extracted the frequency of oscillation. Our Raman beams are co-propagating with the optical dipole trap beams, therefore the direction of the measured dipole trap frequencies is at a 45° angle with respect to the direction of k_R. The kinetic and harmonic terms in the Hamiltonian are

$$\hat{H}_\perp = \frac{1}{2m^\star}k_x^2 + \frac{1}{2m}k_y^2 + \frac{m}{2}[\omega_{x'}^2 x'^2 m + \omega_y'^2 y'^2] \tag{3}$$

with $\mathbf{e}_{x'} = \frac{\mathbf{e}_x + \mathbf{e}_y}{\sqrt{2}}$ and $\mathbf{e}_{y'} = \frac{\mathbf{e}_x - \mathbf{e}_y}{\sqrt{2}}$. For $\omega_{x'} = \omega_{y'}$ a simple rotation yields a trapping

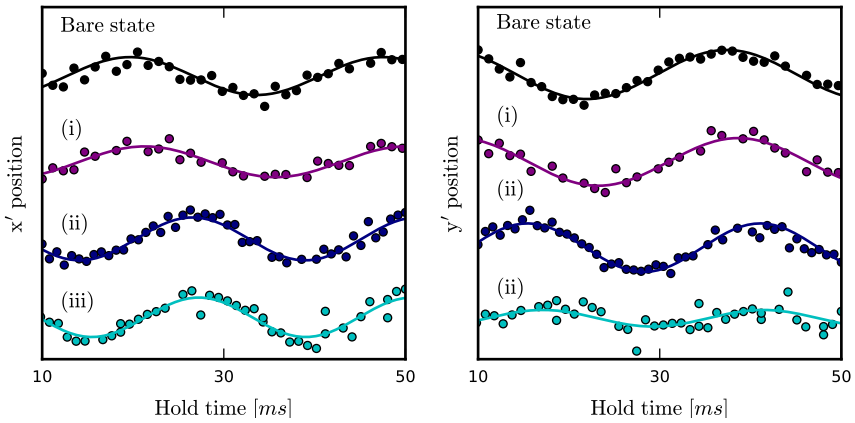

Figure 4. a) Top: Computed cross-sectional cuts of the total potential $V(y)$ (black), effective magnetic field $\boldsymbol{\mathcal{B}}$ (blue) and atomic density $n(y)$ (yellow). Columns correspond to Raman coupling strengths $\hbar = 0.5, 3.5, 5.5\ E_L$ respectively, all with the detuning gradient . Bottom: GPE-computed 2D density distributions $n(x, y)$ using the same parameters. **b)** Second-moment of the momentum distribution as a function of and in our system. Regions with large moments represent large potential well separations that have a synthetic magnetic field localized between the BECs.

frequency along the Raman direction $\omega_x = \sqrt{\omega_x^2 + \omega_y^2}$. Figure 4 shows the dipole oscillations of our BECs along the $\mathbf{e}_{x'}$ and $\mathbf{e}_{x'}$ directions for the three different coupling regimes we are studying, as well as the bare state motion.

We use a not-uniform fast Fourier transform algorithm (NUFFT) which allows us to get the power spectral density for data points that are not necessarily evenly spaced in time as required by regular FFT algorithms. In order to account for missing data points. Figure $nn + 2$ shows the power spectral density (PSD) of the time evolution of each m_f state. Each vertical cut is normalized to the highest peak of the three spin states. We then rescale the units $\hbar\Delta \to \hbar^2 k_x/8m$, extract the highest peaks in the PSD and offset their frequency by $\hbar^2 k_x^2/2m^\star$, finally obtaining the characteristic spin- and momentum- dependent dispersion of a spin orbit coupled system. For the case driven spin-orbit coupling (cases (ii) and (iii)), since the strength of the drive is comparable to the quadratic Zeeman shift,we observe higher frequency components in the dynamics which are in good agreement with Floquet theory.

Our system has dark states at $\Delta = 0$ which can be noted by the missing peaks in the PSD. Since there are eigenstates of the Raman dressed Hamiltonian that never get populated, the time evolution of the system does not have the frequency components related to the missing eigenstates. The presence of the dark states in the system is in good agreement with theory.

4. Discussion

Heating due to scattering of spontaneously emitted photons is always present in our system. It is also well known that heating is present in periodically driven systems, and while it can be minimized by increasing the driving frequency, it in exchange requires more Raman power to tune the spin-orbit coupling strength. The time scales of our pulsing experiments never exceeded 900 μs which is small compared to the lifetime of our system

In conclusion, we can measure the spin and momentum dependent dispersion relation for a spin-1 spin-orbit coupled BEC using our Fourier spectroscopy technique. When used to study periodically driven systems, we are able tp see a rich spectrum that arises from the Floquet quasi-energies. This method is good for any effective three level system with a quadratic branch in the dispersion relation and does not require any additional hardware as it relies only on the Hamiltonian evolution of the system. This technique might prove particularly useful to probe the spin-resolved energy dispersion of atoms in the presence of Rashba spin-orbit coupling using newly proposed schemes to generate this type of coupling without the use of excited states and could lead to a better understanding of new topological matter.

5. Appendix A

5.1. Effective SOC Hamiltonian

The effective spin-orbit coupling Hamiltonian can be derived from the electric dipole Hamiltonian describing the interaction between our Rb atoms and the multiple frequency Raman lasers

$$\hat{H}_{AL}(t) = \left[\Omega_{21}\cos(2k_R x - \omega_{21}t + \phi_1) + \Omega_{31}\cos(2k_R x - \omega_{31}t + \phi_2) + \Omega_{41}\cos(2k_R x - \omega_{41}t + \phi_3)\right]\hat{F}_x \tag{4}$$

where $\Omega_{ij} \propto \vec{E_i} \times \vec{E_j^\star}$ represents the coupling strength associated to each pair of Raman beams and $\omega_{ij} = \omega_i - \omega_j$. We choose the frequencies so that $\omega_{31} + \omega 21$ is at 4 photon resonance with the $m_f = +1 \rightarrow m_f = -1$ transition. We then apply a rotation about the z axis $\hat{U} = e^{i\bar{\omega}t\hat{F}_z}$ where $\bar{\omega} = \frac{\omega_{21}+\omega_{31}}{2}$. For the choice of parameters $\Omega_{21} = \Omega_{31} = \Omega$, $\Omega_{41} = \Omega_0$, and $\omega_{41} = \frac{\omega_{21}+\omega_{31}}{2}$,and after applying the rotating wave approximation (RWA), the Hamiltonian transforms to

$$\begin{aligned}\hat{\tilde{H}}_{AL}(t) = &\frac{1}{2}\{\Omega\cos(2k_R x + \delta\omega t + \phi_1) + \Omega\cos(2k_R x - \delta\omega t + \phi_2) + \Omega_0\cos(2k_R x + \phi_3)\}\hat{F}_x \\ &- \frac{1}{2}\{\Omega\sin(2k_R x + \delta\omega t + \phi_1) + \Omega\sin(2k_R x - \delta\omega t + \phi_2) + \Omega_0\sin(2k_R x + \phi_3)\}\hat{F}_y\end{aligned} \tag{5}$$

we have the freedom of defining the time origin so we can get rid of one phase, lets make it ϕ_3 for convenience. Can I get rid of a second phase? Make $\phi_1 = -\phi_2$

$$\hat{\tilde{H}}_{AL}(t) = [\frac{\Omega_0}{2} + \Omega\cos(\delta\omega t + \phi_1)][\cos(2k_R x)\hat{F}_x - \sin(2k_R x)\hat{F}_y], \tag{6}$$

where we have defined $\delta\omega = \frac{\omega_{31}-\omega_{21}}{2}$. This Hamiltonian term describes a helically precessing effective Zeeman field with amplitude oscillating periodically in time.

The complete Hamiltonian can therefore be written as

$$\hat{H}(t) = \frac{\hbar^2}{2m}\hat{k}^2 + \mu\mathbf{B}_{eff}\cdot\hat{\mathbf{F}} \tag{7}$$

(check units here) with $\mu\mathbf{B}_{eff} = (\frac{\Omega_0}{2}+\Omega\cos(\delta\omega t+\phi_1))(\cos(2k_R x)\mathbf{e}_x - \sin(2k_R x)\mathbf{e}_y) + \Delta_0\mathbf{e}_z$

We can apply a position dependent rotation $\hat{U} = e^{i2k_R x\hat{F}_z}$ transforms our Hamiltonian into the form of Eq. 1 with a time dependent Raman coupling.

$$\begin{aligned}\hat{H}(t) =& \frac{\hbar^2}{2m}(\hat{k} - 2k_R\hat{F}_z)^2 + (\frac{\Omega_0}{2} + \Omega\cos(\delta\omega t))\hat{F}_x \\ &+ \epsilon(\hat{F}_z^2 - \mathbb{I}) + \Delta\hat{F}_z \\ =& \frac{\hbar^2\hat{k}^2}{2m} + \alpha_0\hat{k}\hat{F}_z + 4E_L\mathbb{I} + \frac{\Omega(t)}{2}\hat{F}_x \\ &+ (\epsilon + 4E_L)(\hat{F}_z^2 - \mathbb{I}) + \Delta_0\hat{F}_z\end{aligned} \tag{8}$$

(check factors of 2!)

To get rid of the time dependence in the Hamiltonian and ultimately getting the 'tunable' spin-orbit coupling we can choose a transoformation of the Hamiltonian such that $\hat{U}^\dagger\frac{\partial\hat{U}}{\partial t} = -i\frac{\Omega(t)}{2}\hat{F}_x$. This will be satisfied for

$$\hat{U} = e^{-i\frac{\Omega}{2}\int_0^t\cos(\delta\omega t')dt'} = e^{-i\frac{\Omega}{2\delta\omega}\sin(\delta\omega t)}. \tag{9}$$

Under this time dependent transformation, the time evolution of the system will be given by the Hamiltonian

$$\begin{aligned}\hat{\tilde{H}} =& \hat{U}^\dagger\hat{H}(t)\hat{U} + i\hat{U}^\dagger\frac{\partial\hat{U}}{\partial t} \\ =& \frac{\hbar^2\hat{k}^2}{2m} + \alpha\hat{k}\hat{F}_z + 4E_L\mathbb{I} + \frac{\Omega_0}{2}\hat{F}_x \\ &+ \frac{\tilde{\Omega}}{2}\hat{F}_{xz} + (\tilde{\epsilon} + 4E_L)(\hat{F}_z^2 - \mathbb{I}) + \Delta\hat{F}_z\end{aligned} \tag{10}$$

which is exactly Eq. 2. To arrive to this final form we have transformed the operators that don't commute with $\hat{F}_x$ as

$$\begin{aligned} e^{i\theta\hat{F}_x}\hat{F}_z e^{-i\theta\hat{F}_x} &= \cos\theta\hat{F}_z + \sin\theta\hat{F}_y \\ e^{i\theta\hat{F}_x}\hat{F}_y e^{-i\theta\hat{F}_x} &= -\sin\theta\hat{F}_z + \cos\theta\hat{F}_y \\ e^{i\theta\hat{F}_x}\hat{F}_z^2 e^{-i\theta\hat{F}_x} &= \cos^2\theta\hat{F}_z^2 + \sin^2\theta\hat{F}_y^2 + \sin\theta\cos\theta(\hat{F}_z\hat{F}_y + \hat{F}_y\hat{F}_z). \end{aligned} \tag{11}$$

and neglected the terms oscillating at high frequency

$$\begin{aligned} \cos(\Omega/2\delta\omega\sin(\delta\omega t)) &= J_0(\Omega/2\delta\omega) + 2\sum_{n=1}^{\infty} J_{2n}(\Omega/2\delta\omega)\cos(2n(\delta\omega t)) \\ &\approx J_0(\Omega/2\delta\omega) \\ \sin(\Omega/2\delta\omega\sin(\delta\omega t)) &= 2\sum_{n=0}^{\infty} J_{2n+1}(\Omega/2\delta\omega)\sin((2n+1)(\delta\omega t)) \approx 0, \end{aligned} \tag{12}$$

(verify how large $\delta\omega$ needs to be for this approximation to be valid)

5.2. spin half system

$$\hat{H}_{eff} = \frac{\hbar^2}{2m}(\hat{k} + 2k_R\hat{\sigma}_z)^2 + \frac{\hbar\Omega'}{2}\hat{\sigma}_x + \Delta\hat{\sigma}_z \tag{13}$$

where we have defined an effective coupling between the $m_f = -1$ and $m_f = +1$ states $\Omega' = \tilde{\Omega} + \hbar\Omega_0^2/2(\tilde{\epsilon})$.

5.3. Relative phases

Here put the Hamiltonian with phases.